

Supplementary Information for

Harderian gland development and degeneration in the *Fgf10*-deficient heterozygous mouse

Shiori Ikeda 1, Keita Sato 2, Hirofumi Fujita 2, Hitomi Ono-Minagi 3, Satoru Miyaishi 4, Tsutomu Nohno 1, Hideyo Ohuchi 2*

1 Department of Cytology and Histology, Okayama University Medical School, 2-5-1 Shikata-cho, Kita-ku, Okayama 700-8558, Japan

2 Department of Cytology and Histology, Okayama University Faculty of Medicine, Dentistry and Pharmaceutical Sciences, 2-5-1 Shikata-cho, Kita-ku, Okayama 700-8558, Japan

3 Department of Cytology and Histology, Okayama University Graduate School of Medicine, Dentistry and Pharmaceutical Sciences, 2-5-1 Shikata-cho, Kita-ku, Okayama 700-8558, Japan

4 Department of Legal Medicine, Okayama University Faculty of Medicine, Dentistry and Pharmaceutical Sciences, 2-5-1 Shikata-cho, Kita-ku, Okayama 700-8558, Japan

*Correspondence: ohuchi-hideyo@okayama-u.ac.jp

Supplementary Methods

Quantitative PCR (qPCR)

Embryonic heads at E19 were dissected, divided into right and half halves, and immediately dipped in RNAlater solution (Thermo Fisher Scientific). After 3 days at 4 degrees, RNAlater was removed, and the samples were stored at -80 degrees. When RNA was extracted, NucleoZol solution was added to the frozen tissues, homogenized with a Power Macher II (nippi; Fujifilm Wako, Osaka, Japan), and processed for RNA isolation. cDNA synthesis and qPCR (Fig. S10A, B) were performed as below.

As for E15 samples (Fig. S10C), PFA-fixed embryonic bodies (WT, n = 2; *Fgf10^{+/−}*, n = 3; *Fgf10^{−/−}*, n = 3), frozen for cryosectioning were thawed and washed in PBS three times. The embryonic bodies were homogenized in 1x Protection Reagent (NEB, Ipswich, MA) with a Power Macher II. Total RNA was extracted and purified from 25 mg of homogenized tissues using Monarch Total RNA Miniprep Kit (NEB). Since the tissues were fixed in PFA, proteinase K treatment was performed sufficiently to liberate nuclei acids according to the manufacturer's protocol. After confirmation of RNA integrity, cDNA was synthesized from 1 ug of total RNA in 20 uL volume using FastGene™ Scriptase II (NE-LS65; Nippon Genetics, Tokyo, Japan). After 1:5 dilution, 1 uL of the cDNA solution was used for qPCR in 15 uL volume using THUNDERBIRD Next SYBR™ qPCR Mix (QPX-201; TOYOBO, Osaka, Japan) on LightCycler Nano (Roche, Basel, Switzerland).

As for 19-week Harderian glands (HGs) (Fig. S10D), the tissues were dissected out from the eyeball and immediately dipped in RNA later solution (Thermo Fisher Scientific). The procedures for sample storage, RNA isolation with Nucleozol, cDNA synthesis and qPCR were performed as the same as the above.

qPCR primer sequences and amplicon size are listed in Table S7. Statistical analysis was performed with Igor Pro 9 software (<https://www.wavemetrics.com/products/igorpro>) version 9.0.2.4 (WaveMetrics). The source data for qPCR (Fig. S10) is shown in Table S8.

Supplementary Figures

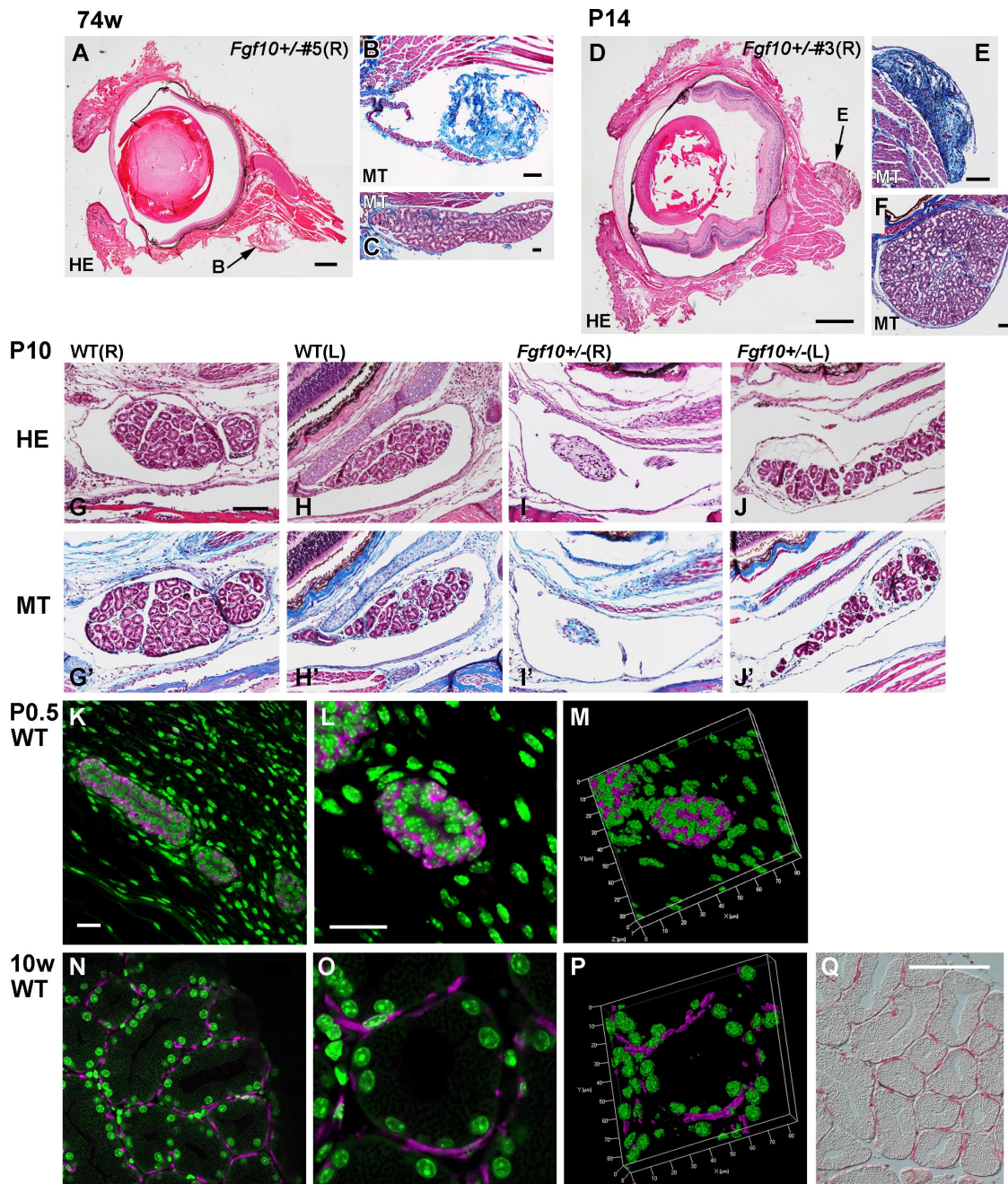


Figure S1. Harderian gland phenotype of the *Fgf10* heterozygous knockout mouse (related to Figure 1): The unilateral gland is often degenerated within 2 weeks from birth.

(A-F) Histology of *Fgf10*^{+/-} eyes with HGs (arrows) of 74-week-old (A-C) and P14 (D-F) mice. Hematoxylin-eosin (HE) (A, D) or Masson trichrome (MT) (B, C, F, F) stain was performed. Right (A, B, D, E) and left (C, F) sides are shown. Marked fibrosis is observed in (B, E). (G-J, G'-J') Histology of the developing HGs of WT and *Fgf10*^{+/-} mice at P10. Sections of right (G, G', I, I') and left (H, H', J, J') HGs are shown. HE stain (G-J) and corresponding MT stain (G'-J') were performed. (K-Q) Immunohistochemistry of pancytokeratin. Panels (K-P) show localization of pancytokeratin (magenta) and nuclei (green) in WT P0.5 (K-M) or 10-week (N-P) HGs as revealed by confocal microscopy (K, L, N, O: Z-stack images; M, P: 3D images). Panel (Q) shows a differential interference contrast (DIC) microscopic image of the HG tissue at 10 weeks. Scale bars: 0.4 mm (A, D), 100 µm (B, C, E, F, G-J, G'-J', Q), 20 µm (K, N, L, O).

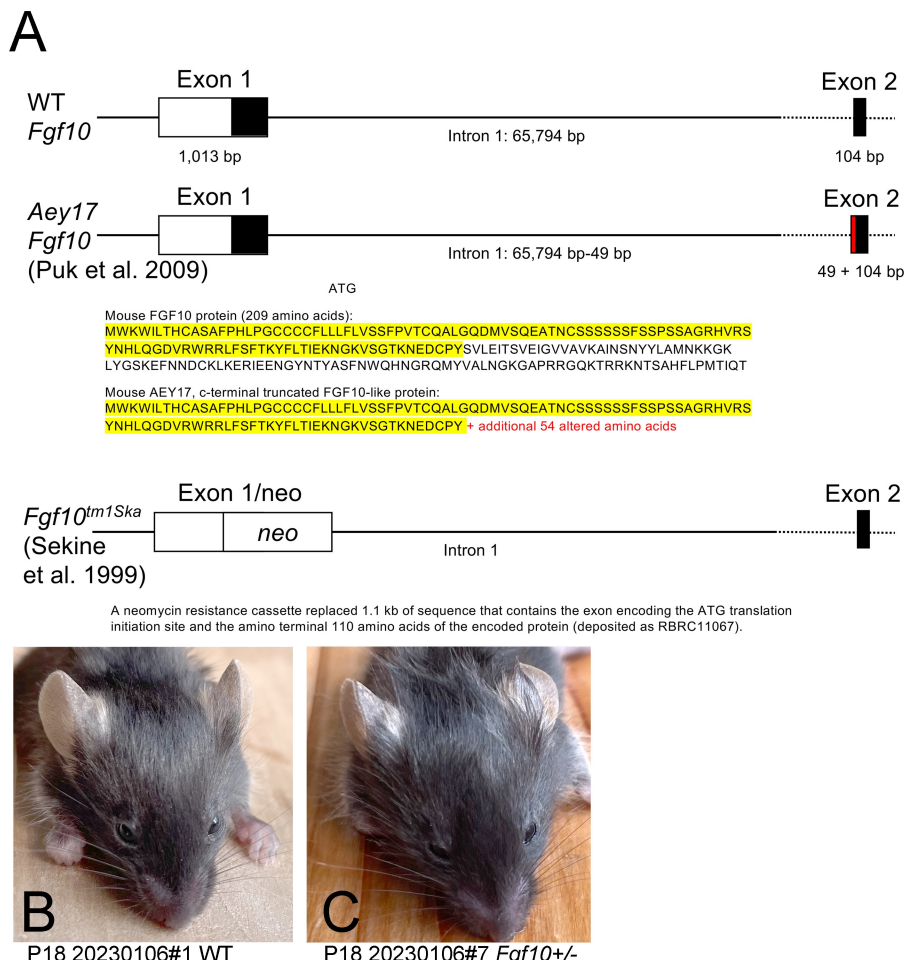


Figure S2. Structure of wild-type and mutant *Fgf10* exons (A) and photos of the face of wild-type (B) and *Fgf10*^{+/−} (C) mice at P18 in this study. (A) The mouse *Fgf10* gene has three exons, and the schema depicts the first two exons. The length of exon 1 and intron 1 is after the Ensembl database (ENSMUST0000022246.9).

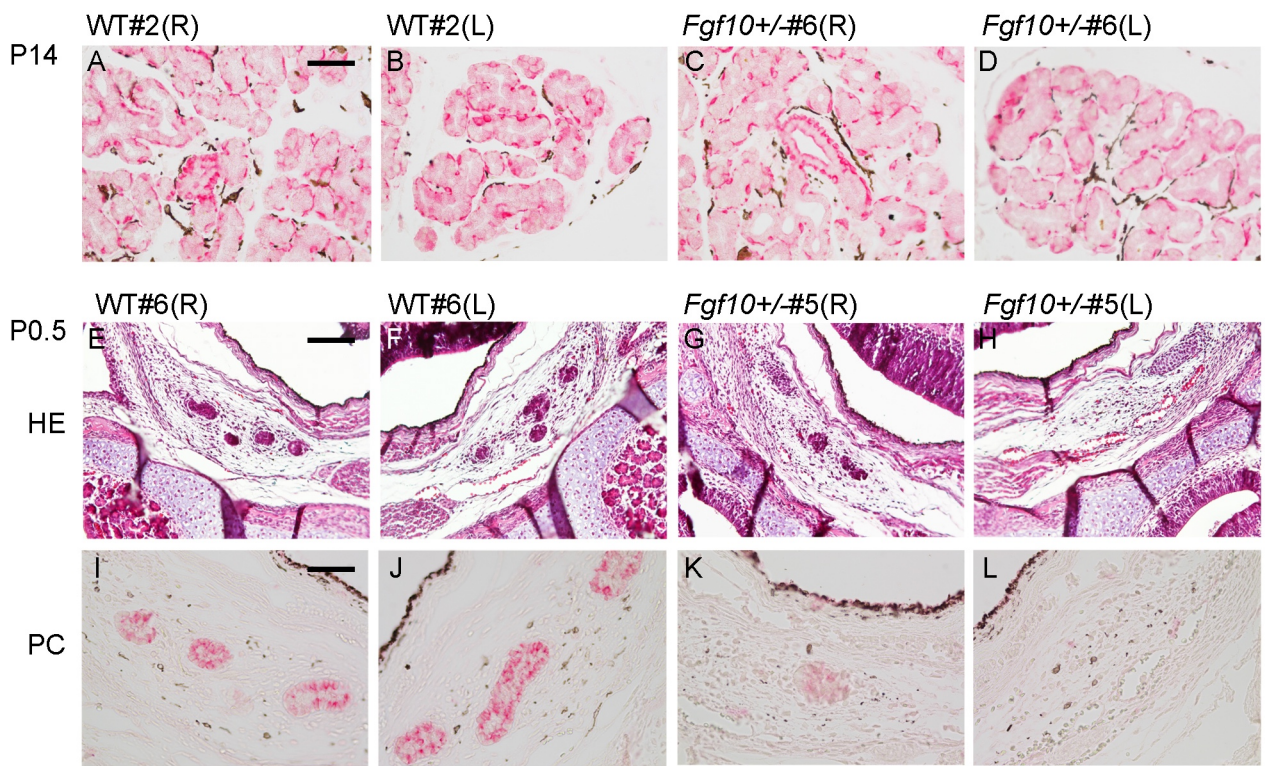


Figure S3. Immunohistochemistry of pancytokeratin, related to Figures 1 and 2. (A-D) Sections of HGs on both sides from a WT (A, B) and an *Fgf10*^{+/-} (C, D) mice at P14 were used. Localization of pancytokeratin in HGs is seen in red. Interstitial melanocytes are observed in dark brown. (E-H) Histology (HE stain) of a WT and an *Fgf10*^{+/-} developing HGs of P0.5 mice as indicated. (I-L) Immunohistochemistry of pancytokeratin (shown in red). Sections of HGs on both sides from the WT (E, F, I, J) and the *Fgf10*^{+/-} (G, H, K, L) mice were used. Scale bars: 50 μ m (A-D, I-L), 100 μ m (E-H).

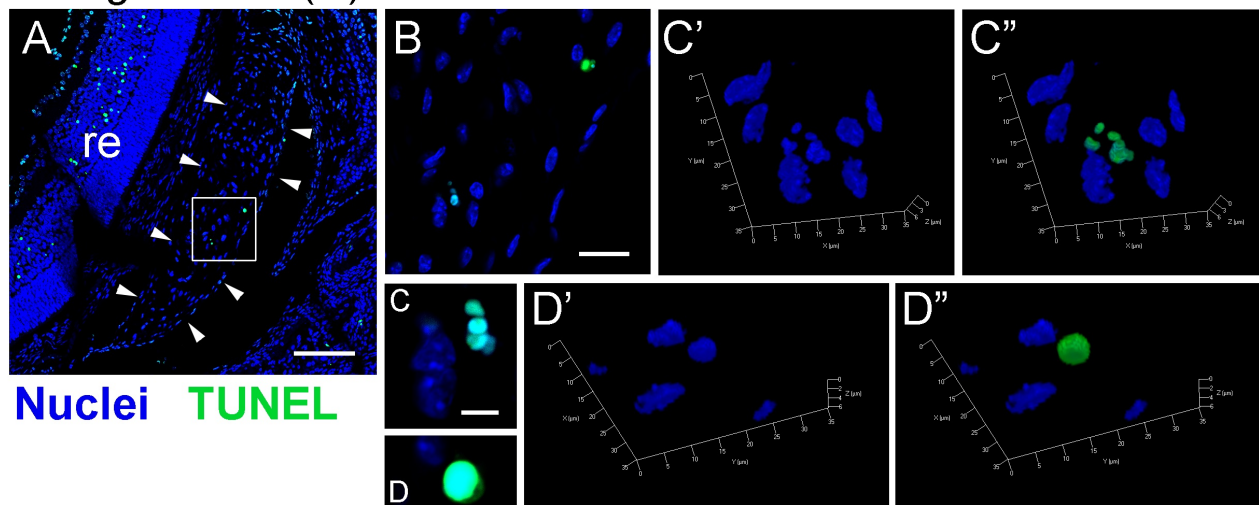
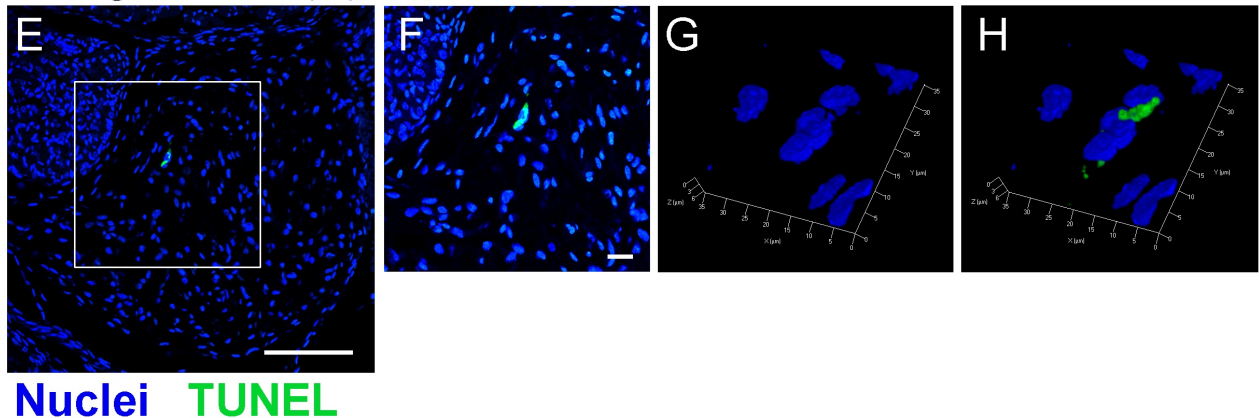
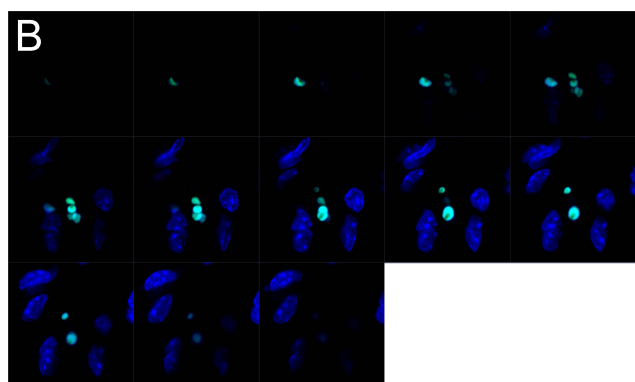
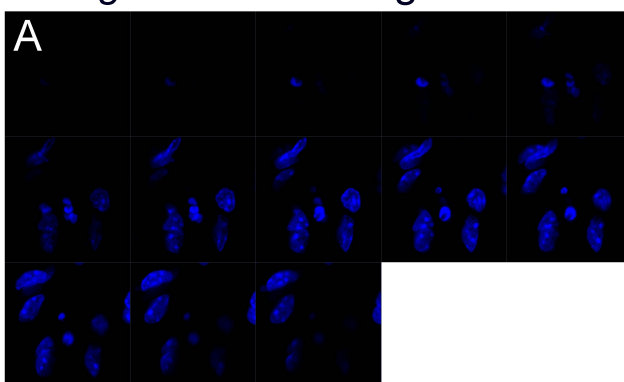
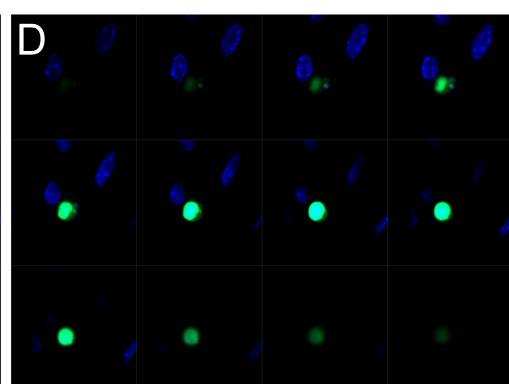
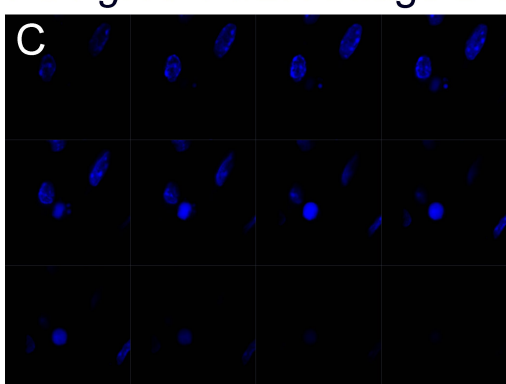
P6 *Fgf10+/-#2(R)*

P6 *Fgf10+/-#3(R)*


Figure S4. Additional and original data for Fig. 1Z-AA'. Since confocal microscopic images were taken with an inverted light microscope, the photos were mirror-imaged as shown here. Fig. 1AA is shown as the original one, panel H. Boxed area in (A) is enlarged in (B), where two TUNEL-positive portions are observed. The left is enlarged in (C-C''), and the right is enlarged in (D-D''). TUNEL-positive signals (green) are merged with fragmented (C', C'') or pyknotic (D', D'') nuclei (blue). Boxed area in (E) is enlarged in (F). TUNEL positive signal (green in H) is partly merged with fragmented nuclei (blue in G). Scale bars: 50 µm (A), 20 µm (B, F), 5 µm (C, D), 100 µm (E).

P6 *Fgf10+/-#2R* Image C series



P6 *Fgf10+/-#2R* Image D series



P6 *Fgf10+/-#3R* Images G and H

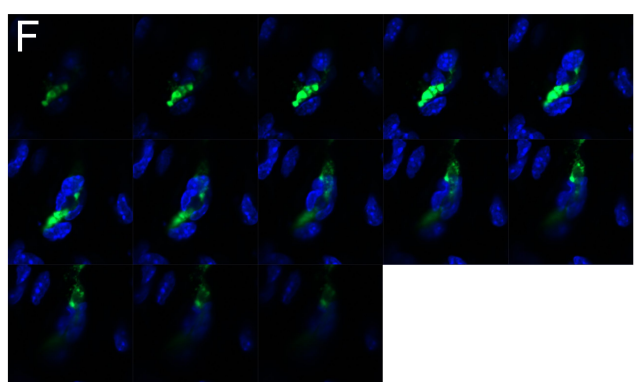
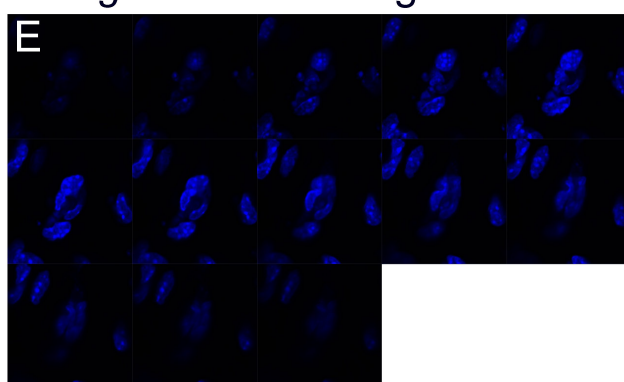


Figure S5. Original source data for Fig. 1Z', Z'', AA', and Fig. S4C-C', D-D'', G, H.

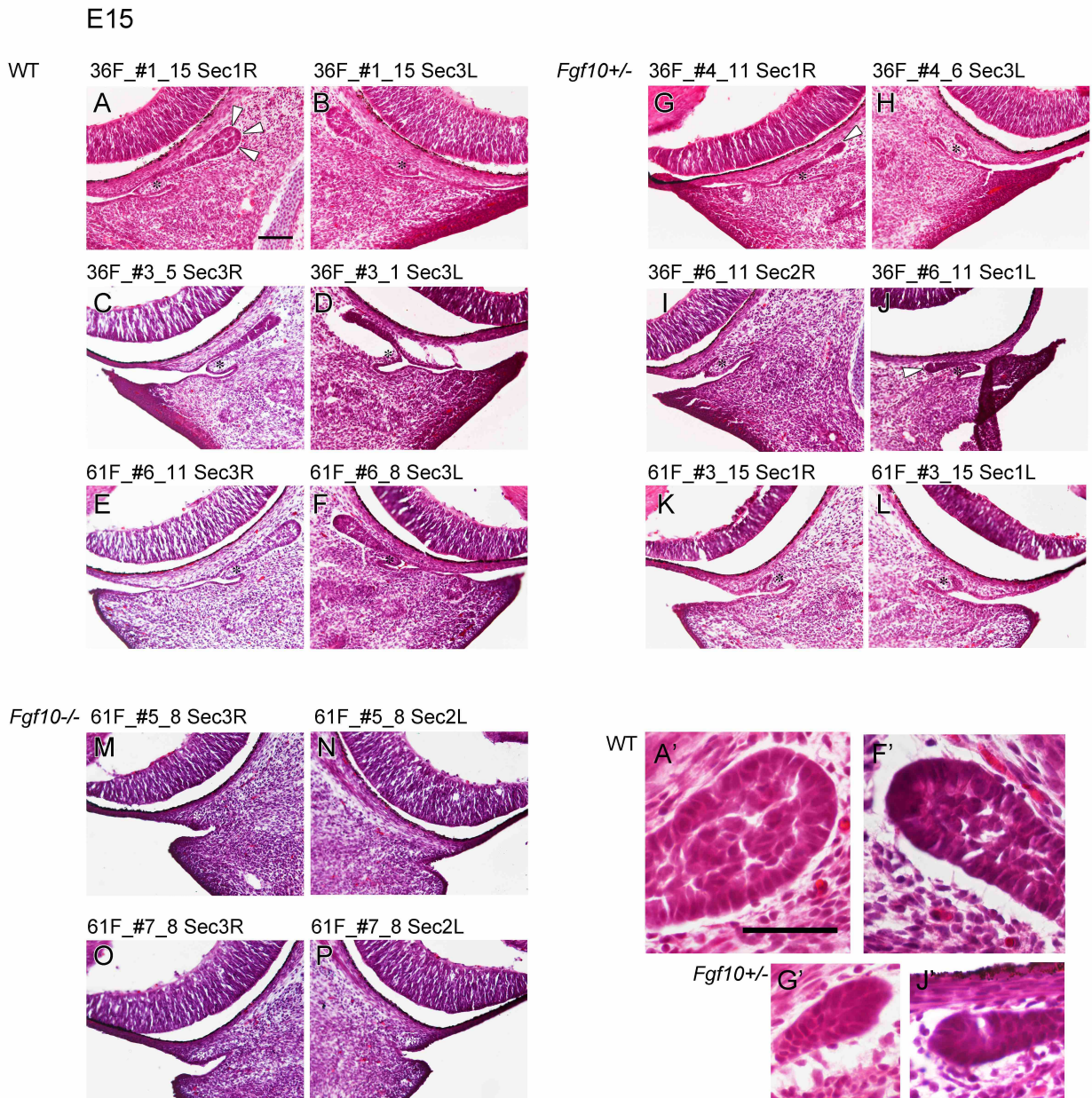


Figure S6. The early histology of invaginating surface ectoderm at E15, related to Fig. 2C', D'. Arrowheads in (A) shows the tip of the invaginating epithelium along the eyeball, multilayered with columnar and cuboidal cells. Compare with the arrowhead in (G), indicating a smaller tip of the elongating glandular epithelium. The tips of the elongating glandular cells in (A, F, G, J) are enlarged in (A', F', G', J'), respectively. Histology of *Fgf10^{-/−}* samples on right (R) and left (L) sides are also shown in (M-P) (n = 2). Primordia for the nictitating membrane do not protrude well. Scale bars: 100 µm (A-P), 50 µm (A', F', G', J').

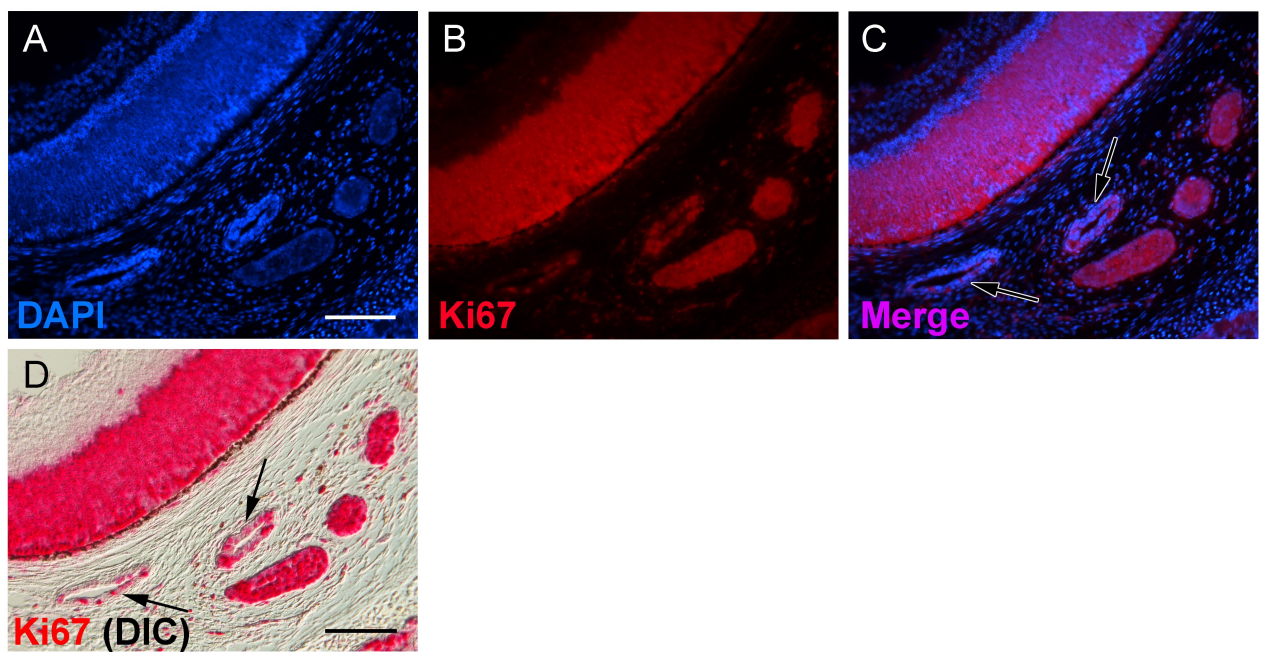


Figure S7. Ki67 expression is decreased in the cavitating HG primordia. Supporting data for Fig. 2F. Fluorescence microscopic images (A-C) and differential interference contrast image (D) of E19 mouse HGs. Localization of Ki67 protein is visualized with Vector Red. Arrows in (C, D) shows cavitating HG cells, in which fewer Ki67-positive cells are observed than in other three proliferating glandular portions. Scale bars: 100 μ m (A-C), 100 μ m (D).

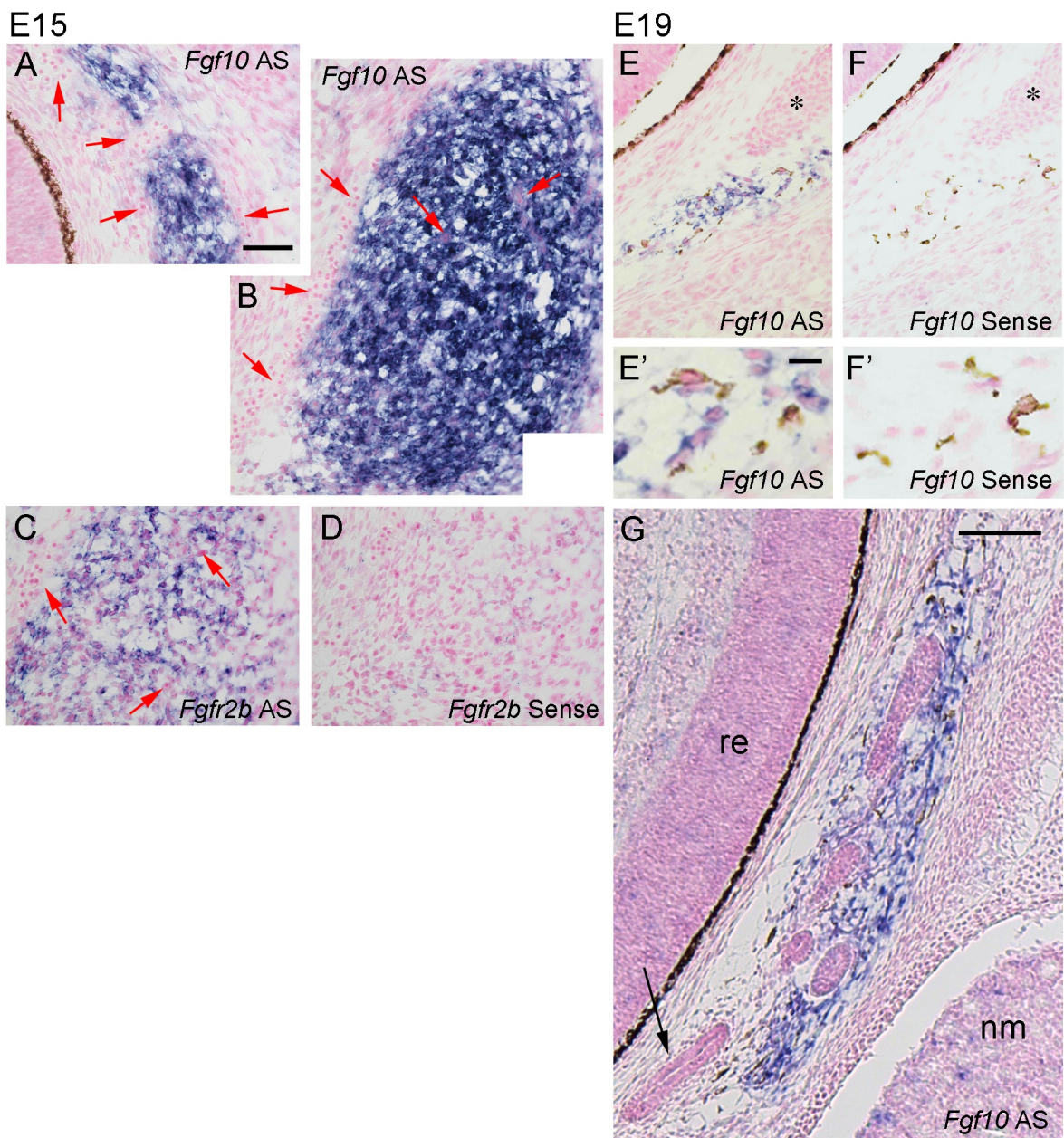


Figure S8. In situ hybridization of *Fgf10* (E15, E19) and *Fgfr2b* (E15) in the WT mouse head mesenchyme, related to Figures 3 and 4. (A, B) Two horizontal levels of the E15 WT head are shown, rostral (upper) (A) and caudal (lower) (B) levels. In panel (A), arrows show round cells abutting the *Fgf10*-expressing mesenchymal cells. In (B), arrows show the similar round cells, possibly hemangioblasts, abutting and intermingling with the *Fgf10*-expressing mesenchymal cells. (C) *Fgfr2b* expression in the *Fgf10*-expressing periocular mesenchymal domain. Arrows show the round cells without *Fgfr2b* expression, abutting and intermingling with the *Fgfr2b*-expressing mesenchymal cells. (D) Hybridized with an *Fgfr2b* sense probe as a negative control. (E) No *Fgf10* expression in the mesenchymal melanoblasts. (F) Hybridized with an *Fgf10* sense probe as a negative control. Asterisks in (E, F) show the developing cartilage core of the nictitating membrane. Magnified view of Harderian melanoblasts in (E, F) are shown in (E', F'), respectively. (G) No *Fgf10* expression in the surrounding mesenchyme of HGs in tubulogenesis (arrow). Scale bars: 50 µm (A-F), 10 µm (E', F'), 100 µm (G).

E19 *Fgf10* +/- (26F_#7)

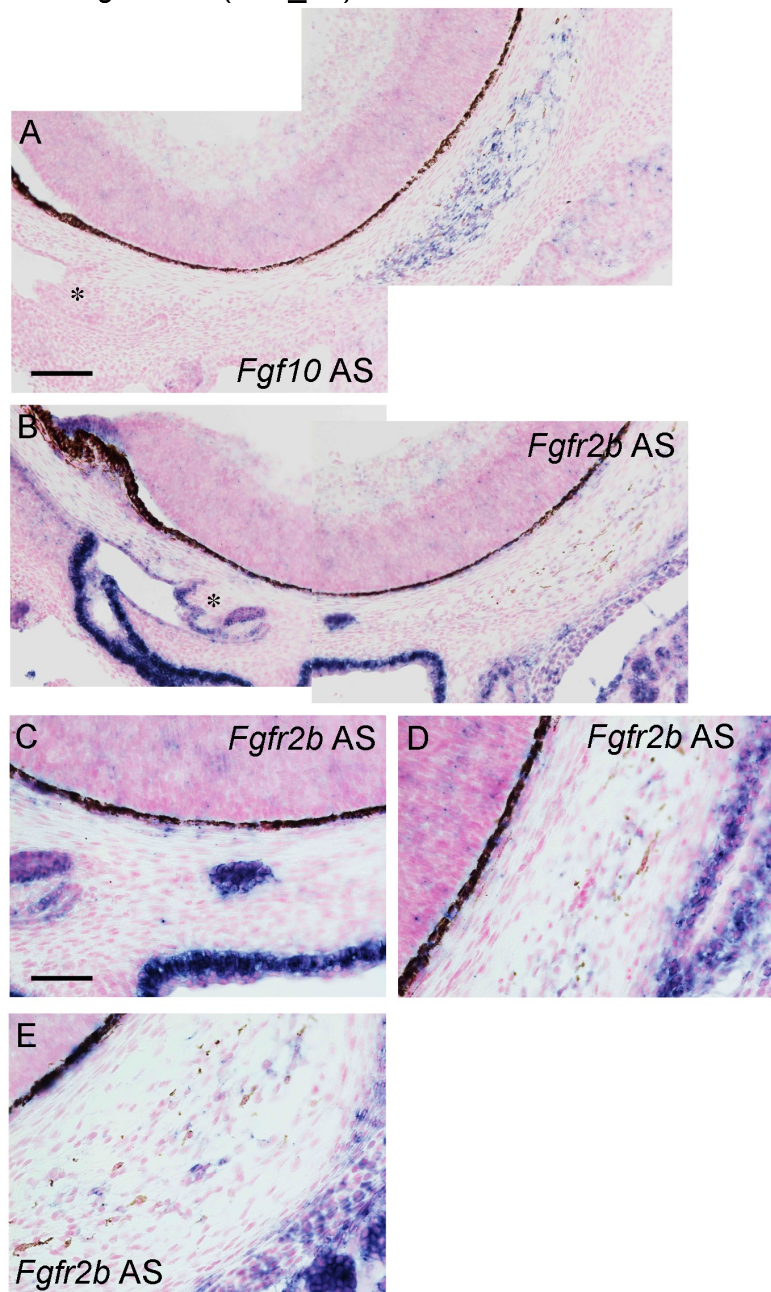


Figure S9. In situ hybridization of *Fgf10* and *Fgfr2b* in the E19 *Fgf10⁺⁻* mouse HG primordium, related to Figure 4. Asterisks in (A, B) show the developing nictitating membrane. (A) High magnification of Fig. 4I. *Fgf10* is expressed in the HG mesenchyme not to contain developing glandular epithelial cells. (B) High magnification of Fig. 4K. *Fgfr2b* expression indicates that HG cells did not reach the HG mesenchyme. (C) High magnification of panel (B). Different expression levels of *Fgfr2b* are observed depending on the epithelia. (D) A more rostral (upper level) section of (C). A small population of cells without *Fgfr2b* expression is found in the HG mesenchyme. (E) A more caudal (lower level) section of panel (C). A few *Fgfr2b*-expressing cells are scattered in the HG mesenchyme. Scale bars: 100 μ m (A, B), 50 μ m (C-E).

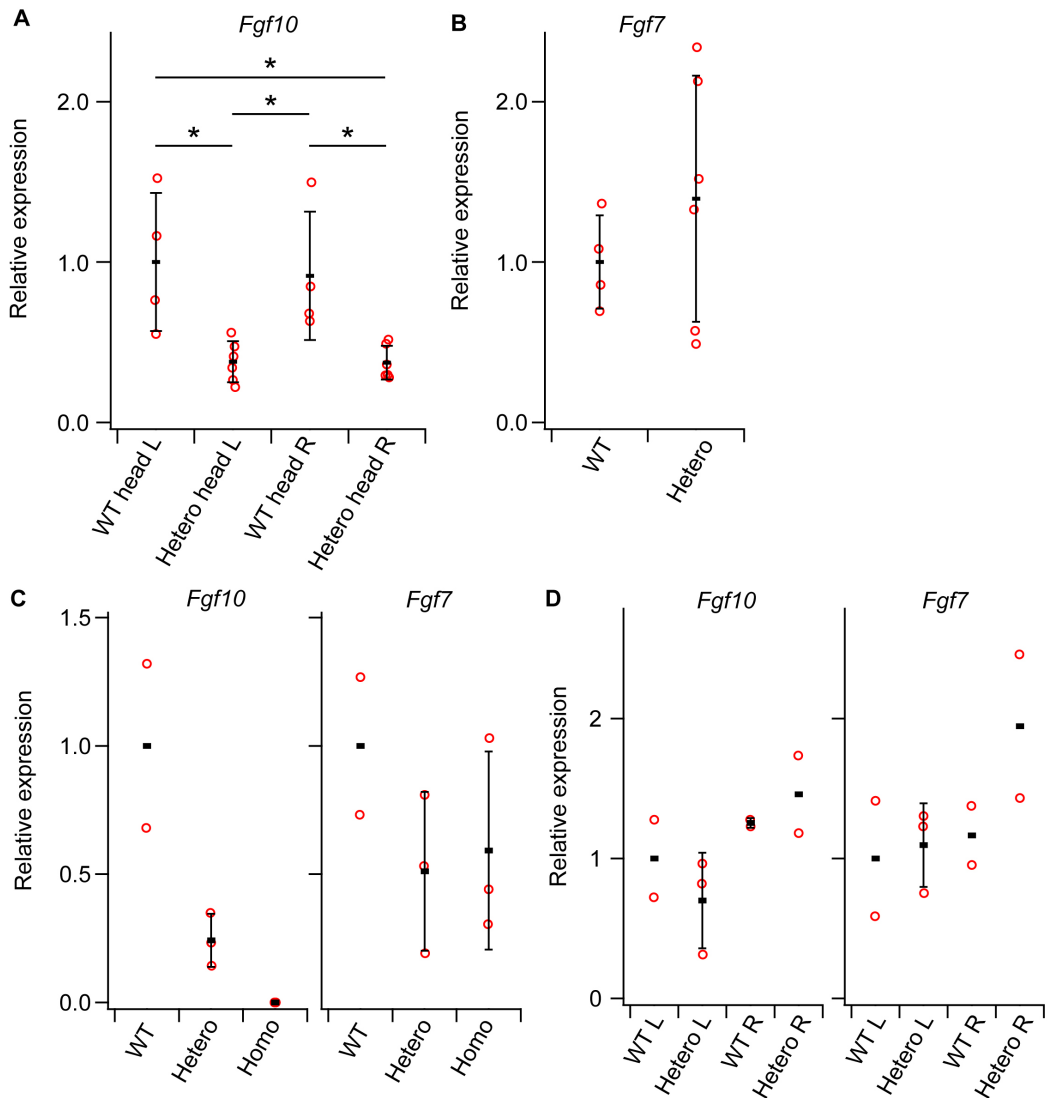


Figure S10. Relative expression levels of *Fgf10* and *Fgf7* in wild-type, *Fgf10*^{+/-}, and *Fgf10*^{-/-} embryos and adult Harderian tissues as shown by qRT-PCR. Mean and standard deviation are indicated. Red plots show the individual data points. (A) Relative expression levels of *Fgf10* in wild-type (WT) and *Fgf10*^{+/-} (Hetero) heads at E17.5. Total RNA was extracted, and cDNA were synthesized from left (L) and right (R) heads separately and processed for qPCR. n = 4 for WT and n = 6 for *Fgf10*^{+/-} mice were used. (B) Relative expression levels of *Fgf7* in WT and *Fgf10*^{+/-} heads at E17.5. n = 4 for WT, n = 6 for *Fgf10*^{+/-}-mice were used. (C) Relative expression levels of *Fgf10* and *Fgf7* in WT, *Fgf10*^{+/-} and *Fgf10*^{-/-} (Homo) embryos at E15. n= 2 for WT, n = 3 for *Fgf10*^{+/-}, and n = 3 for *Fgf10*^{-/-} embryos were used. In the *Fgf10*^{+/-} embryos, *Fgf10* expression tends to be decreased than wild-type. In the *Fgf10*-null embryos, *Fgf10* is not expressed at all. *Fgf7* expression levels did not tend to be upregulated in the *Fgf10*^{+/-} or *Fgf10*-null embryos. (D) Relative expression levels of *Fgf10* and *Fgf7* in WT and *Fgf10*^{+/-}, right and left Harderian glands at 19 weeks. n = 2 for left WT, n = 3 for left *Fgf10*^{+/-}, n = 2 for right WT, and n = 2 for right *Fgf10*^{+/-} HGs (as one right *Fgf10*^{+/-} HG was degenerated). *P < 0.05, nonparametric two-sided Wilcoxon rank-sum test with Benjamini–Hochberg correction.

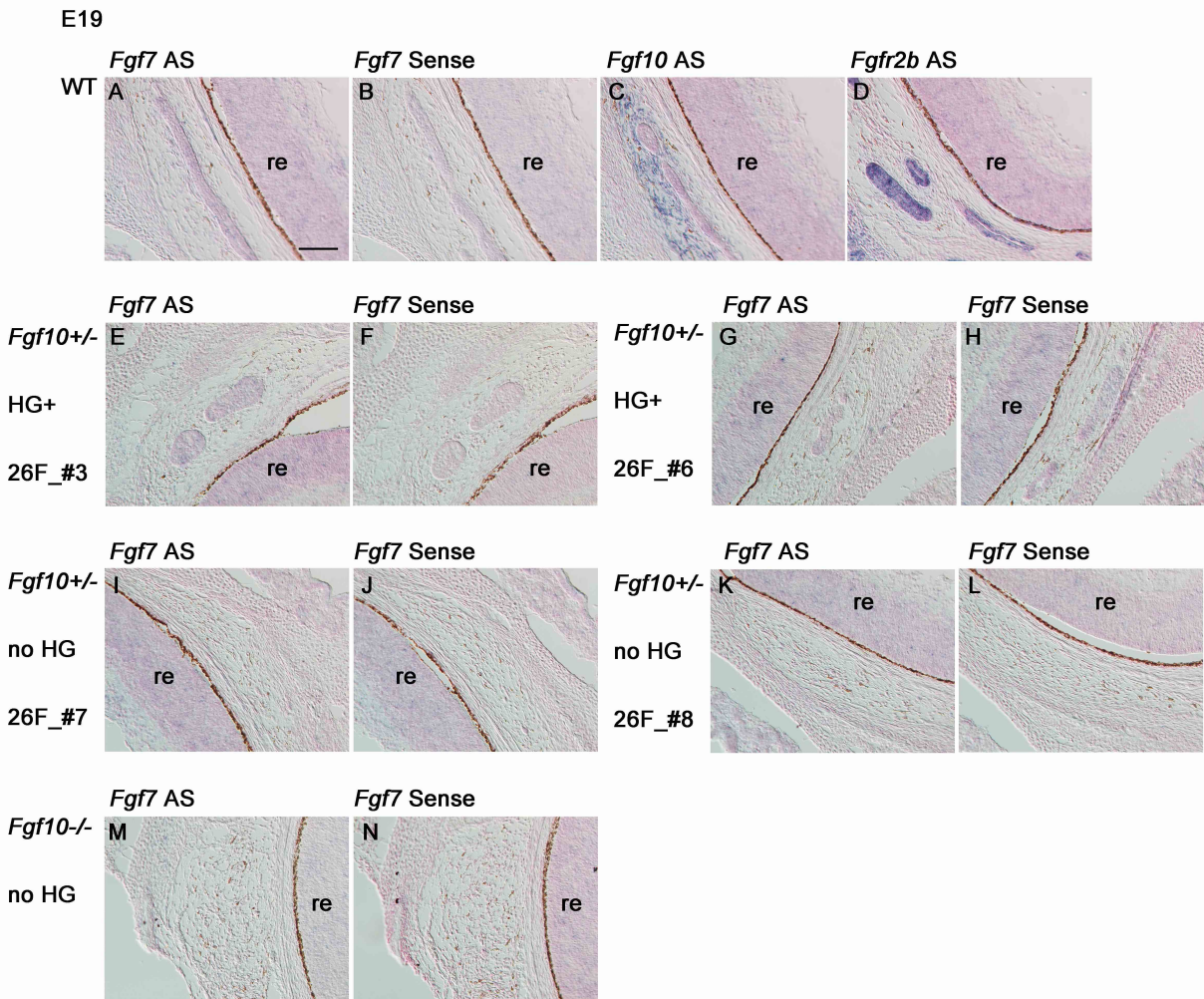


Figure S11. *Fgf7* is not expressed in the wild-type, *Fgf10^{+/−}*, or *Fgf10^{−/−}* developing Harderian tissues at E19 as revealed by *in situ* hybridization. Expression of *Fgf10* and *Fgfr2b* is shown in (C, D) as experimental controls. High magnification and additional data for Fig. 4C-H. Scale bar: 100 μ m (A-N).

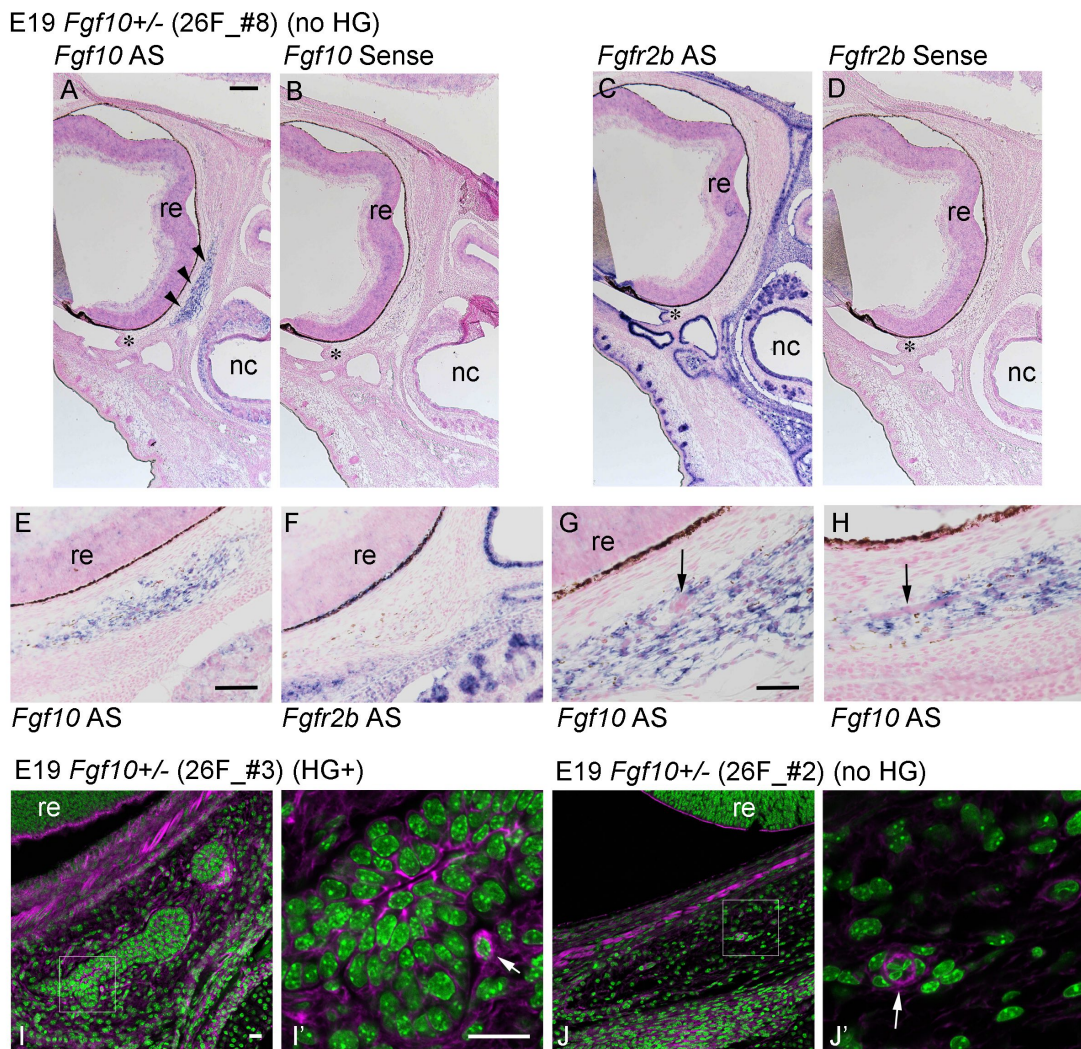


Figure S12. In situ hybridization of *Fgf10* and *Fgfr2b*, and localization of F-actin in other E19 *Fgf10*^{+/−} HG primordia, related to Figure 4. Horizontal sections are shown. Nasal cavity (nc) is shown downward. In this *Fgf10*^{+/−} embryo (26F_#8), there were no HG epithelial cells in the periocular mesenchyme, judging from *Fgfr2b* expression. (A) *Fgf10* is expressed in the HG mesenchyme without glandular epithelia. (B) Hybridized with an *Fgf10* sense probe as a negative control. (C) There are no *Fgfr2b*-expressing epithelial cells within the periocular mesenchyme. (D) Hybridized with an *Fgfr2b* sense probe as a negative control. (E-H) High magnification of the HG mesenchyme is shown. (E) A more caudal (lower level) section of panel (A). (F) A more rostral (upper level) section of (C). (G) High magnification of (A). Arrow shows round cells populated in the HG mesenchyme. (H) A more rostral (upper level) section of (A). Arrow shows thin tubular cells populated in the HG mesenchyme. (I, I', J, J') Confocal micrographs of frozen sections after phalloidin (magenta) and nuclear (green) stain. Boxed area in (I, J) are enlarged in (I', J'), respectively. (I') Localization of F-actin is relatively intense at the apical domain facing the HG lumen in the *Fgf10*^{+/−} embryo (26F_#3) with developing HG. A cell in the HG mesenchyme (arrow) has relatively intense F-actin localization in the cytoplasm. (J) This *Fgf10*^{+/−} embryo (26F_#2) has no HG development. In the HG mesenchyme, there is a round F-actin localization, enlarged in (J'). Cells (arrow in J') are aligned in rosette formation. Localization of F-actin is also observed in the apical domain of the neural retina (re), vascular smooth muscles of the choroid, and developing extraocular muscles in (I, J). Scale bars: 2 μm (A-D), 100 μm (E, F), 50 μm (G, H), 20 μm (I and J, I' and J').

Supplementary Tables

Table S1. Phenotypes of Harderian glands in wild-type (WT) and *Fgf10+/-* mice at 74 weeks of age.

Abbreviations: R, right; L, left; HG, Harderian gland; M, male; w, weeks; PFA, paraformaldehyde,

Definition: 3+, well developed; 2+ developed but less than wild-type male one; 1+ present but obviously small; absent, could not be found; degenerated, markedly small and blackened.

Body weight (g)	Animal #	Genotype	Sex	Age	Fixation date	Fixative	R)HG	L)HG	
41	3M	WT	♂	74w	2022.10.20	FEKETE	3+	3+	
44.2	4M	WT					3+	3+	
49.5	7M	WT			2023.1.12	FEKETE	3+	3+	
43.3	12M	WT			2023.8.9	4%PFA	3+	3+	
35.8	13M	WT					3+	3+	
37.6	14M	WT					3+	3+	
26.4	2M	<i>Fgf10+/-</i>			2022.10.20	FEKETE	degenerated	3+	
51.5	5M	<i>Fgf10+/-</i>			2023.1.12	FEKETE	degenerated	3+	
40.8	6M	<i>Fgf10+/-</i>					3+	3+	
43.4	9M	<i>Fgf10+/-</i>			2023.5.10	4%PFA	3+	3+	
51.1	11M	<i>Fgf10+/-</i>			2023.10.12		degenerated	3+	
39.3	16M	<i>Fgf10+/-</i>					3+	3+	
54	2F	WT	♀	74w	2023.1.18	FEKETE	3+	3+	
39.5	3F	WT			2023.5.10		3+	3+	
41.1	10F	WT			2023.8.9		2+	2+	
62.6	11F	WT			2023.10.12		3+	3+	
55.2	14F	WT			2023.5.10	4%PFA	3+	3+	
35.5	4F	<i>Fgf10+/-</i>					degenerated	3+	
33.2	5F	<i>Fgf10+/-</i>					3+	degenerated	
33	9F	<i>Fgf10+/-</i>					degenerated	3+	
39.3	7F	<i>Fgf10+/-</i>					degenerated	degenerated	
51.9	12F	<i>Fgf10+/-</i>					3+	3+	
33	13F	<i>Fgf10+/-</i>			2023.10.12		3+	3+	

Table S2. Phenotypes of Harderian glands in wild-type (WT) and <i>Fgf10+/-</i> mice at postnatal day 18 (P18).																	
Abbreviations: R, right; L, left; HG, Harderian gland; PFA, paraformaldehyde.																	
Definition: degenerated, markedly small and blackened.																	
Body weight (g)	Animal #	Genotype	Sex	Age	Fixation date	Fixative	R)HG (weight, mg)	R)HG weight / body weight	L)HG (weight, mg)	L)HG weight / body weight							
5.7	26F_1	WT	♂	2023.1.6	P18	4% PFA	3.1	developed	0.5439	3.5	developed	0.614					
5.0	26F_2	WT					3.2	developed	0.64	2.7	developed	0.54					
4.8	26F_3	WT					1.7	developed	0.3542	2.9	developed	0.6042					
4.2	26F_6	WT					3.5	developed	0.8333	3.6	developed	0.8571					
2.5	26F_4	<i>Fgf10+/-</i>					2.5	developed	1	1	degenerated	0.4					
4.5	26F_5	<i>Fgf10+/-</i>		2023.6.5			1.4	degenerated	0.3111	4.1	developed	0.9111					
3.4	26F_7	<i>Fgf10+/-</i>					3.4	developed	1	1.1	degenerated	0.3235					
5.5	40F_1	WT					2.2	developed	0.4	2.8	developed	0.5091					
7.4	40F_2	WT					4.4	developed	0.5946	4.3	developed	0.5811					
7.9	40F_3	WT					4.6	developed	0.5823	4.5	developed	0.5696					
6.8	40F_4	WT	♂				3.8	developed	0.5588	3.4	developed	0.5					
5.8	40F_5	<i>Fgf10+/-</i>					3.7	developed	0.6379	1	degenerated	0.1724					
6.7	40F_6	<i>Fgf10+/-</i>					2.9	developed	0.4328	1.6	degenerated	0.2388					
6.3	40F_7	<i>Fgf10+/-</i>					4.4	developed	0.6984	0.9	degenerated	0.1429					
7.7	40F_8	<i>Fgf10+/-</i>					3.7	developed	0.4805	4	developed	0.5195					

Table S3.		Phenotypes of Harderian glands in wild-type (WT) and <i>Fgf10+/-</i> mice at early postnatal days (P0.5 to P14).				
		Abbreviations: R, right; L, left; HG, Harderian gland; PFA, paraformaldehyde.				
		Definition: degenerated, markedly small and blackened.				
Animal #	Genotype	Age	Fixation date	Fixative & treatment	R)HG	L)HG
2	WT	P0.5	2022.12.15	4%PFA, decalcified	developed	developed
4	WT				developed	developed
6	WT				developed	developed
11	WT				developed	developed
1	<i>Fgf10+/-</i>				developed	no HG
3	<i>Fgf10+/-</i>				developed	developed
5	<i>Fgf10+/-</i>				developed	no HG
10	<i>Fgf10+/-</i>				developed	no HG
4	WT	P1	2022.3.31	4%PFA	developed	developed
6	WT				developed	developed
2	<i>Fgf10+/-</i>				no HG	no HG
8	<i>Fgf10+/-</i>				developed	developed
1	<i>Fgf10+/-</i>	P2.5	2023.9.8	4%PFA, decalcified	delayed	developed
2	WT			4%PFA, decalcified	developed	developed
3	WT			4%PFA, decalcified	developed	developed
4	WT			4%PFA, decalcified	developed	developed
5	<i>Fgf10+/-</i>			4%PFA, decalcified	developed	delayed
1	WT	P6	2023.9.1	4%PFA, decalcified	developed	developed
2	<i>Fgf10+/-</i>			4%PFA, decalcified	degenerated	developed
3	<i>Fgf10+/-</i>			4%PFA, decalcified	degenerated	developed
5	WT			4%PFA, decalcified	developed	developed
1	WT	P10	2023.3.29	4%PFA, decalcified	developed	developed
3	<i>Fgf10+/-</i>				degenerated	developed
1	WT	P14	2022.9.14	4%PFA	developed	developed
2	WT				developed	developed
4	<i>Fgf10+/-</i>				developed	degenerated
6	<i>Fgf10+/-</i>				developed	developed
2_1	WT	2022.11.18	FEKETE		developed	developed
2_2	WT				developed	developed
2_3	<i>Fgf10+/-</i>				degenerated	developed
2_4	WT				developed	developed

Table S4. Antibody and reagent list.

Antibodies	Dilution	Antigen retrieval	Company	Catalog #	IgG
anti-E-cadherin	50	boiling in citrate buffer (0.1M, pH6)	BD Bioscience	610181	mouse
anti-Pancytokeratin	200	boiling in citrate buffer (0.1M, pH6)	Abcam	ab86734	mouse
anti-Ki67	4500	boiling in citrate buffer (0.1M, pH6)	Abcam	ab15580	rabbit
anti-mouse IgG, Alexa Fluor 488	1000	N. A.	Thermo Fisher Scientific	A11029	goat
anti-rabbit IgG, Alexa Fluor 594	1000	N. A.	Thermo Fisher Scientific	A11037	goat
<hr/>					
Reagents	Dilution	Concentration	Company	Catalog #	
DAPI	5000	1mg/ mL	Dojindo	340-0791	
Hoechst 33342	1000	1mg/ mL	Nacalai Tesque	04929-82	
Rhodamine Phalloidin	50	N. A.	Thermo Fisher Scientific	R415	
Mouse IgG isotype control	no dilution	0.5 ug/ mL	Thermo Fisher Scientific	08-6599	
Normal rabbit IgG	11000	11 mg/ mL	Fujifilm Wako	148-09551	
ImmPRESS Duet Double Staining HRP/AP Polymer Kit	N. A.	N. A.	Vector Laboratories	MP-7714	
ImmPRESS-AP Horse Anti-Rabbit IgG Polymer Detection Kit	N. A.	N. A.	Vector Laboratories	MP-5401	
DeadEnd™ Colorimetric TUNEL System	N. A.	N. A.	Promega	G7360	
DeadEnd™ Fluorometric TUNEL System	N. A.	N. A.	Promega	G3250	
<hr/>					
N. A.: not applicable					

Table S5. Oligonucleotide sequences for conventional ISH probes used in this study.				
Primers for cDNA cloning				
Primer name	Primer/DNA sequences (5'->3')	Gene name	Accession No.	Amplicon size (bp)
mmu_Fgfr2_Fw	ATGGGATTACCGTCCACGTGGAGATATGGA	<i>Fgfr2</i>	NM_201601.2	2181
mmu_Fgfr2_Rv	TCATGTTTAACACTGCCCTTATGTGTGG			
mmu_Fgf10_Fw	CAACAAAACGCCAGCCGCA	<i>Fgf10</i>	NM_008002.5	1279
mmu_Fgf10_Rv	CTATGTTGGATCGTCATGGGGAGG			
mmu_Fgf7_Fw	AAGGTTAACAGTTGGAAAGAGCGACGA	<i>Fgf7</i>	NM_008008.4	734
mmu_Fgf7_Rv	TTAGGTTATGCCATAGGAAGAAAA			
Primers for other purposes				
Primer name	Primer/DNA sequences (5'->3')	Usage		
T7 primer	GTAATACGACTCACTATAGGG	Sequencing cDNAs inserted in pBluescriptII KS+ and preparation of riboprobe synthesis template		
T3 primer	AATTAACCCCTACTAAAGGAA	Sequencing cDNAs inserted in pBluescriptII KS+ and preparation of riboprobe synthesis template		
under_T7prom_pBSIIKSplus	CGCTCTAGAACTAGTGGATC	Preparation of riboprobe synthesis template for Fgf10 and Fgf7		
under_T3prom_pBSIIKSplus	AGGTCGACGGTATCGATAAG	Preparation of riboprobe synthesis template for Fgf10 and Fgf7		
SP6_under_T7prom_pBSIIKSplus	CATTTAGGTGACACTATAGAACGCTCTAGAACTAGTG	Preparation of riboprobe synthesis template for Fgf10 and Fgf7		
SP6_under_T3prom_pBSIIKSplus	CATTTAGGTGACACTATAGAACGCTCGACGGTATCG ATAAGC	Preparation of riboprobe synthesis template for Fgf10 and Fgf7		
Fgfr2_seq_Fw	TGCAAGGTTACAGCGATGC	Sequencing isoform specific region of Fgfr2b cDNA clones		

Table S6. Oligonucleotide sequences and other information for SABER-FISH in this study.

Table S6. Oligonucleotide sequences and other information for SABER-FISH in this study.			
Hairpins and branches	Nucleotide sequence (5'->3')	Usage	Reference
Oligo name			
h.67.31.tail	ATTATTCAGGGCCTTTGGCCAGTGAATAAATTATGTGATTTTTT	Remap primer sequence in probe from no.67 to no.31	Kishi et al. 2019
h.31.31.tail	ATTATTCAGGGCCTTTGGCCAGTGAATAAATAGTGAATAATTTTTT	Extension of probe or branch oligos	Kishi et al. 2019
h.27.27.tail	ACATCATCATGGGCCTTTGGCCATGTGATGTATGATGTTTTTT	Extension of probe or branch oligos	Kishi et al. 2019
h.28.28.tail	ACAACTTAACGGGCCTTTGGCCCTTAAAGTTGTAAAGTTGTTTTT	Extension of probe or branch oligos	Kishi et al. 2019
h.60.60.tail	AACAACTATGGGCCTTTGGCCATAGTTAGTTAGTTAGTTGTTTTT	Extension of probe or branch oligos	Kishi et al. 2019
h.73.73.tail	ATTCTTAATCGGGCCTTTGGCCGATAGGAATGATTAGGAATTTTTT	Extension of probe or branch oligos	Kishi et al. 2019
31*.31*.31*.31*.27	AGTGAATAATAGTGAATAATAGTGAATAATAGTGAATAATTICATCAT	branch for signal amplification in SABER	Kishi et al. 2019
27*.27*.27*.28	ATGATGATGTATGATGTATGATGTTCAACTAAC	branch for signal amplification in SABER	Kishi et al. 2019
60*.60*.60*.60*.73	ATAGTTAGTTAGTTAGTTAGTTAGTTAGTTAGTTAGTTCTAATC	branch for signal amplification in SABER	Kishi et al. 2019
28*.488	/SATTO488N/TGTTAGATTGTGTTAGTTG	Fluorescent detection	Kishi et al. 2019
73*.565	/SATTO565N/TTGATTAGGAATGATTAGGAAT	Fluorescent detection	Kishi et al. 2019
Clean.G	CCCCGAAAGTGGCCTGGGCTTGGCCGAGGCCACTTTCG	Removal of dGTP contaminated in primer exchange reaction	Kishi et al. 2019

Pool name	Sequence
mmu_Fgf10_5utr_cds.67	TGTGAAGTCTTCCGAAAGCCACTTCTGTTGGGGttTCACATAAT
mmu_Fgf10_5utr_cds.67	GTCTCTTGGAGTTGTCAGAACTGGAGGCAGCTGCTttTCACATAAT
mmu_Fgf10_5utr_cds.67	TCTCTGCAGAGTCCCAGCCTGCTGCCACTAAAAttTCACATAAT
mmu_Fgf10_5utr_cds.67	CAGGACGGTGAACAAAACCCAAAGTGGTGGGGTgttTCACATAAT
mmu_Fgf10_5utr_cds.67	ACTCCTTCTCACCATGTTAGATGCAAAAGAGGTCTGAAAttTCACATAAT
mmu_Fgf10_5utr_cds.67	GAAC TG GT GGT GTC GGT CACCAGAGCTCTCGCTCttTCACATAAT
mmu_Fgf10_5utr_cds.67	TAAC TT CT AGGAAGGAC CGG CT GC CT GT CC CT CG CT CttTCACATAAT
mmu_Fgf10_5utr_cds.67	TACGGATCTGCCAGAACGAGTGCAACACATCCttTCACATAAT
mmu_Fgf10_5utr_cds.67	ACATACTGGAAGGGTAAGACCTGCTGCAGGGCAGAttTCACATAAT
mmu_Fgf10_5utr_cds.67	AACTCTCGGCACTGAAATTGTCATCAGAAGGAttTCACATAAT
mmu_Fgf10_5utr_cds.67	AGGCACAATGTGTCAGTATCCA TTCCACATTGACTGAttTCACATAAT
mmu_Fgf10_5utr_cds.67	AGCTTGGCAGGTGACAGGGAACGAAGACACCAAAAttTCACATAAT
mmu_Fgf10_5utr_cds.67	CTTGGAGGTGATTGAGCTCGCACATGCCTCCCttTCACATAAT
mmu_Fgf10_5utr_cds.67	GGTGAAGGAGAACAGCCTCTCCAGCGGACATCTCttTCACATAAT
mmu_Fgf10_5utr_cds.67	TGACCTTGCCTCTCAATCGTAGGAAAGTACTTttTCACATAAT
mmu_Fgf10_5utr_cds.67	CTGTTGATGGCTTGACGGCAACAACTCCGATTTCttTCACATAAT
mmu_Fgf10_5utr_cds.67	TGAGCCATAGAGTTCCCTTCTGTCATGGCTAAGTAATTttTCACATAAT
mmu_Fgf10_5utr_cds.67	GCTGCCAGTTAAAAGATGCATAGGTGTTGATCCATTTCttTCACATAAT
mmu_Fgf10_5utr_cds.67	TCCATTCAATGCCACATACATTGCCTGCCATTGTttTCACATAAT
mmu_Fgf10_5utr_cds.67	GATCGTCATGGGGAGGAAGTGAGCAGAGGTGTTTttTCACATAAT
mmu_Fgf10_5utr_cds.67	GGTTGTACTGCA TCCACCAACAGTGT TTTCTATGTTGttTCACATAAT

Pool name	Sequence		
mmu_Fgfr2b.60	GTAATCCCACCTGCACACTCTTCTGAGACCATGGGttACTAACTAT		
mmu_Fgfr2b.60	CCTGGTCCTCTCCATATCTCCACGTGGACGttACTAACTAT		
mmu_Fgfr2b.60	CCCCAGCTGACCATGGTCACAGTGCCAATCttACTAACTAT		
mmu_Fgfr2b.60	CAGGGACAAGGTTGCCATGGTGACCAAGACttACTAACTAT		
mmu_Fgfr2b.60	TATCCTCAACTAAACTGAAGGAGGGCCGGGttACTAACTAT		
mmu_Fgfr2b.60	CAGGGACAGCGTGGAGCCGCTCTCCATCTttACTAACTAT		
mmu_Fgfr2b.60	CCCAGCCGGACAGCGGAACCTCACAGTGTttACTAACTAT		
mmu_Fgfr2b.60	TTTTAACCAACCTCATTGTGGCGTTGGATTCCCttACTAACTAT		
mmu_Fgfr2b.60	CAATGCGATGCTCCTGCTTAAACTCCTCCCGttACTAACTAT		
mmu_Fgfr2b.60	GACCACACTTCCATAATAAGGCTCAGTGCCTGGTttACTAACTAT		
mmu_Fgfr2b.60	CAGGCAGGTGTAGTTGCCTTGTCTGACGGttACTAACTAT		
mmu_Fgfr2b.60	TAGGTGTGGTTGATGGACCCGTATTCAATTCTCCACttACTAACTAT		
mmu_Fgfr2b.60	ACCGTGGAGGCATTGCAGGCAGTCCAGCTTttACTAACTAT		
mmu_Fgfr2b.60	TTGCAGACAAACTCCACATCCCCTCCGACCttACTAACTAT		
mmu_Fgfr2b.60	TGGATGTGGGGCTGGGCATCGCTGTAAACCttACTAACTAT		
mmu_Fgfr2b.60	TACTGCCGTTCTTCCACGTGCTTGATCCACttACTAACTAT		
mmu_Fgfr2b.60	TGAGGTAGGGCAGCCATCAGGCCGTATTttACTAACTAT		
mmu_Fgfr2b.60	AGCCAGCACTCTGCATTGGAGCTATTATCCCCttACTAACTAT		
mmu_Fgfr2b.60	TATACTCCCCAGCATCCATCTCGTCACATTGAACAGttACTAACTAT		
mmu_Fgfr2b.60	GTGAGCCAGGCAGACTGGTGGCCTGCCCTATA TttACTAACTAT		
mmu_Fgfr2b.60	ATAGCTATCTCAGATAATCTGGGAAGCCGTGATCTttACTAACTAT		
mmu_Fgfr2b.60	ACCATGCAGGCAGATTAGAAGACCCCTATGCAtttACTAACTAT		
mmu_Fgfr2b.60	CGTGGTCTTCATTCCGCAAAAGATGACTGTCACCttACTAACTAT		
mmu_Fgfr2b.60	TGGCTGGCTGCTGAAGTCTGGCTTGGTttACTAACTAT		
mmu_Fgfr2b.60	GGGGATGCGCTGGTCAGCTGTGCACAGCttACTAACTAT		
mmu_Fgfr2b.60	TTATCCTCACCAAGCGGGGTGTTGGAGTTCAttACTAACTAT		
mmu_Fgfr2b.60	GGGTGTCCGCTGTTGAGGACAGACCGCGTTttACTAACTAT		
mmu_Fgfr2b.60	CAACTCATACTCGGAGACCCCTGCTAGCATCGttACTAACTAT		
mmu_Fgfr2b.60	GGTTTGTCTTATCGATTCCACTGCTTCAGCCATGttACTAACTAT		
mmu_Fgfr2b.60	ATCTTCACTGCCACGGTGACCGCCTCCTGttACTAACTAT		
mmu_Fgfr2b.60	TCCATCTCTGATACCAGATCAGACAGGTCCCTCTGttACTAACTAT		
mmu_Fgfr2b.60	GGGCTGGAGGTATTCCGGAGGTGCTTttACTAACTAT		
mmu_Fgfr2b.60	ATGTCATAGGAGTACTCCATGCCAGGTGCCttACTAACTAT		
mmu_Fgfr2b.60	AAGGTCACTGCTCCTCGGGGACACGGTTAtttACTAACTAT		
mmu_Fgfr2b.60	AGCTGGTAGGTGCAGGACACCAAGTCCTGttACTAACTAT		
mmu_Fgfr2b.60	TTTTGGGAAGCCAAGTACTCCATGCCTCTAGCCttACTAACTAT		
mmu_Fgfr2b.60	TCACATTGTTCTGTTACCAACACGTTCTGGCAGCttACTAACTAT		
mmu_Fgfr2b.60	ATAGTAGTCTATGTTGTTGATATCCCTGGCCAGGCCAtttACTAACTAT		
mmu_Fgfr2b.60	AAAAGGGCTTCAGGAGCCATCCACTGACTGttACTAACTAT		
mmu_Fgfr2b.60	CCCCTAAAGTAAAGATCTCCACATTAACACCCCGAAtttACTAACTAT		
mmu_Fgfr2b.60	AAAAGTTCCACGGGAATCCCTGGGTAGGttACTAACTAT		
mmu_Fgfr2b.60	AGTTGGTGGCTGTCCATCCTGTGTCCTttACTAACTAT		
mmu_Fgfr2b.60	CAACTGCTGAATGTGGGTCTGTGAGGGTACAtttACTAACTAT		
mmu_Fgfr2b.60	TGGTTGTGAGAGTCAGAATTCGATCCAAGTCTTCGACttACTAACTAT		
mmu_Fgfr2b.60	TGTGTCGGGGTAACTAGGAGAATACTGTTGAGAGGttACTAACTAT		
mmu_Fgfr2b.60	ACAGAACATCGTCCCTGAAGAACAGAGCTCCTttACTAACTAT		
mmu_Fgfr2b.60	CAGGGTTCATAAGGCATGGGGCTGGAGAAAACttACTAACTAT		
mmu_Fgfr2b.60	TTAACACTGCCATTATGTGTGGACTGAGGCAGAtttACTAACTAT		

Remapping information in PER reaction				
Primer sequence of mmu_Fgf10_5utr_cds.67 was remapped to no.31.				
Primer sequences of mmu_Fgfr2b.60 and branches were not remapped.				
Applied probes and branches in each hybridization step				
Target genes	probe hyb	1st branch hyb	2nd branch hyb	Fluorescent oligo hyb
<i>Fgf10 & Fgfr2b</i>	mmu_Fgf10_5utr_cds.31 (extended) mmu_Fgfr2b.60 (extended)	31*.31*.31*.31*.27 (extended) 60*.60*.60*.60*.73 (extended)	27*.27*.27*.28 (extended) not applicable	28*.488 73*.565

Table S7. qPCR primers used in this study.

Gene name	Forward (5'-3')	Reverse (5'-3')	Amplicon size (bp)	Reference
<i>Fgf10</i>	CGGGACCAAGAATGAAGACT	GCAACAACCTCCGATTCCAC	69	Finburgh et al., 2023, Invest Ophthal Vis Sci
<i>Fgf7</i>	ATAGAACAGGTGCGACAAGG	CAGACAGCAGACACGGAAC	105	Du et al. 2016, Gene Expr Patterns
<i>Gapdh</i>	AGGTTGTCTCCTGCGACTTCA	TGGTCCAGGGTTCTTACTCC	294	Liu et al., 2008, Biochem J

References

1. Du, W.; Prochazka, J.; Prochazkova, M.; Klein, O.D. Expression of FGFs during early mouse tongue development. *Gene Expr Patterns* **2016**, *20*, 81-87, DOI:10.1016/j.gep.2015.12.003.
2. Finburgh, E.N.; Mauduit, O.; Noguchi, T.; Bu, J.J.; Abbas, A.A.; Hakim, D.F.; Bellusci, S.; Meech, R.; Makarenkova, H.P.; Afshari, N.A. Role of FGF10/FGFR2b Signaling in Homeostasis and Regeneration of Adult Lacrimal Gland and Corneal Epithelium Proliferation. *Invest Ophthalmol Vis Sci* **2023**, *64*, 21, DOI:10.1167/iovs.64.1.21.
3. Liu, X.; Li, P.; Liu, P.; Xiong, R.; Zhang, E.; Chen, X.; Gu, D.; Zhao, Y.; Wang, Z.; Zhou, Y. The essential role for c-Ski in mediating TGF-beta1-induced bi-directional effects on skin fibroblast proliferation through a feedback loop. *Biochem J* **2008**, *409*, 289-297, DOI:10.1042/BJ20070545.

Table S8. Source data for qPCR.

For Figure S10A:

Sample	Target gene	Cq	ΔCq	$2^{-\Delta Cq}$	$2^{-\Delta\Delta Cq}$	Group	mean $2^{-\Delta Cq}$	sdev $2^{-\Delta Cq}$	mean $2^{-\Delta\Delta Cq}$	sdev $2^{-\Delta\Delta Cq}$
sample no.2 WT head L	Gapdh	17.9816								
sample no.5 WT head L	Gapdh	16.9181								
sample no.7 WT head L	Gapdh	16.9352								
sample no.10 WT head L	Gapdh	19.1147								
sample no.2 WT head R	Gapdh	17.5064								
sample no.5 WT head R	Gapdh	17.5469								
sample no.7 WT head R	Gapdh	15.975								
sample no.10 WT head R	Gapdh	18.6673								
sample no.1 Hetero head L	Gapdh	16.8165								
sample no.3 Hetero head L	Gapdh	17.048								
sample no.4 Hetero head L	Gapdh	16.2154								
sample no.6 Hetero head L	Gapdh	16.1016								
sample no.8 Hetero head L	Gapdh	18.135								
sample no.9 Hetero head L	Gapdh	16.8556								
sample no.1 Hetero head R	Gapdh	17.5569								
sample no.3 Hetero head R	Gapdh	17.1665								
sample no.4 Hetero head R	Gapdh	17.3831								
sample no.6 Hetero head R	Gapdh	17.8526								
sample no.8 Hetero head R	Gapdh	17.3779								
sample no.9 Hetero head R	Gapdh	16.7449								
sample no.2 WT head L	Fgf10	31.5277	13.5461	8.36004E-05	0.551624549 WT head L		0.0001516	6.53317E-05	1	0.431082
sample no.5 WT head L	Fgf10	29.9971	13.0789	0.00011557	0.762570713					
sample no.7 WT head L	Fgf10	29.4055	12.4704	0.000176217	1.16274223					
sample no.10 WT head L	Fgf10	31.1956	12.0809	0.000230825	1.523064119					
sample no.2 WT head R	Fgf10	30.8575	13.351	9.57056E-05	0.631498984 WT head R		0.0001385	6.05963E-05	0.914032	0.399836
sample no.5 WT head R	Fgf10	30.7921	13.2452	0.000102991	0.679571657					
sample no.7 WT head R	Fgf10	28.9014	12.9264	0.000128455	0.847591179					
sample no.10 WT head R	Fgf10	30.7726	12.1054	0.000226945	1.497466189					
sample no.1 Hetero head L	Fgf10	31.4179	14.6014	4.02296E-05	0.265448786 Hetero head L		5.739E-05	1.94029E-05	0.378712	0.128027
sample no.3 Hetero head L	Fgf10	31.2874	14.2394	5.1704E-05	0.341161506					
sample no.4 Hetero head L	Fgf10	30.1839	13.9685	6.23808E-05	0.411610779					
sample no.6 Hetero head L	Fgf10	29.868	13.7664	7.17637E-05	0.473521901					
sample no.8 Hetero head L	Fgf10	31.6603	13.5253	8.48154E-05	0.559642006					
sample no.9 Hetero head L	Fgf10	31.7221	14.8665	3.34759E-05	0.220885778					
sample no.1 Hetero head R	Fgf10	31.7217	14.1549	5.48231E-05	0.361742424 Hetero head R		5.657E-05	1.59469E-05	0.373254	0.105223
sample no.3 Hetero head R	Fgf10	30.8813	13.7148	7.43743E-05	0.490748067					
sample no.4 Hetero head R	Fgf10	31.8227	14.4396	4.5002E-05	0.296939336					
sample no.6 Hetero head R	Fgf10	31.4934	13.6408	7.82911E-05	0.516592305					
sample no.8 Hetero head R	Fgf10	31.8352	14.4573	4.44552E-05	0.2933308					
sample no.9 Hetero head R	Fgf10	31.2684	14.5235	4.24606E-05	0.280169825					

Table S8. Source data for qPCR.

For Figure S10B:

Sample	Target gene	Cq	ΔCq	$2^{-\Delta Cq}$	$2^{-\Delta\Delta Cq}$	Group	mean $2^{-\Delta Cq}$	sdev $2^{-\Delta Cq}$	mean $2^{-\Delta\Delta Cq}$	sdev $2^{-\Delta\Delta Cq}$
sample no.2 WT head	Gapdh	16.7813								
sample no.5 WT head	Gapdh	20.9939								
sample no.7 WT head	Gapdh	17.2176								
sample no.10 WT head	Gapdh	18.7568								
sample no.1 Hetero head	Gapdh	17.1271								
sample no.3 Hetero head	Gapdh	16.9754								
sample no.4 Hetero head	Gapdh	18.1147								
sample no.6 Hetero head	Gapdh	19.1906								
sample no.8 Hetero head	Gapdh	18.1532								
sample no.9 Hetero head	Gapdh	18.9948								
sample no.2 WT head	Fgf7	29.0172	12.2359	0.00021	0.6938261	WT head	0.0002988	8.70E-05	1	0.291145
sample no.5 WT head	Fgf7	32.588	11.5941	0.00032	1.082529					
sample no.7 WT head	Fgf7	29.1469	11.9293	0.00026	0.8581177					
sample no.10 WT head	Fgf7	30.0159	11.2591	0.00041	1.3655306					
sample no.1 Hetero head	Fgf7	29.8681	12.741	0.00015	0.4888723	Hetero head	0.00041704	0.0002294	1.39569	0.767629
sample no.3 Hetero head	Fgf7	29.49	12.5147	0.00017	0.5719067					
sample no.4 Hetero head	Fgf7	28.5974	10.4827	0.0007	2.3389245					
sample no.6 Hetero head	Fgf7	29.8099	10.6193	0.00064	2.1275485					
sample no.8 Hetero head	Fgf7	29.4532	11.3	0.0004	1.3273015					
sample no.9 Hetero head	Fgf7	30.0996	11.1048	0.00045	1.5195914					

Table S8. Source data for qPCR.

For Figure S10C:

Table S8. Source data for qPCR.

For Figure S10D:

Table S9.		List of animals/embryos shown in Figures.				
Age/stage	Genotype	Sex	Animal #	Figure #	Experiments	
74w	WT	♂	3M	Figure 1A, B, E~G	HE, Masson	
74w	<i>Fgf10+/-</i>	♂	11M	Figure 1C, C', D, H~J	HE, Masson	
74w	<i>Fgf10+/-</i>	♂	5M	Figure S1A~C	HE, Masson	
P18	<i>Fgf10+/-</i>	♂	40F_7	Figure 1N~Q	Masson, TUNEL	
P18	WT	♂	26F_1	Figure S2B	Photography of the face	
P18	<i>Fgf10+/-</i>	♀	26F_7	Figure S2C	Photography of the face	
P14	WT		1	Figure 1R, S	Pancytokeratin	
P14	<i>Fgf10+/-</i>		4	Figure 1T, U	Pancytokeratin	
P14	WT		2	Figure S3A, B	Pancytokeratin	
P14	<i>Fgf10+/-</i>		6	Figure S3C, D	Pancytokeratin	
P14	<i>Fgf10+/-</i>		3 (2_3)	Figure S1D~F	HE, Masson	
P10	<i>Fgf10+/-</i>		3	Figure S1G~J'	HE, Masson	
P6	<i>Fgf10+/-</i>		2	Figure 1V, W	HE	
P6	<i>Fgf10+/-</i>		2	Figure 1Z~Z"; Figure S4A~D"; Figure S5A~D	TUNEL	
P6	<i>Fgf10+/-</i>		3	Figure 1X, X', Y	HE	
P6	<i>Fgf10+/-</i>		3	Figure 1AA, AA'; Figure S4E-H; Figure S5E, F	TUNEL	
P0.5	WT		11	Figure 2I, J	HE	
P0.5	WT		6	Figure S3E, F	HE	
P0.5	<i>Fgf10+/-</i>		10	Figure 2K, L	HE	
P0.5	<i>Fgf10+/-</i>		5	Figure S3G, H	HE	
P0.5	WT		11	Figure 2M, N	Pancytokeratin	
P0.5	WT		6	Figure S3I, J	Pancytokeratin	
P0.5	<i>Fgf10+/-</i>		10	Figure 2O, P	Pancytokeratin	
P0.5	<i>Fgf10+/-</i>		5	Figure S3K, L	Pancytokeratin	
E19	<i>Fgf10+/-</i>		26F_3(HG+)	Figure 4E, F	ISH for <i>Fgf7</i>	
E19	<i>Fgf10+/-</i>		26F_3(HG+)	Figure S11E, F	ISH for <i>Fgf7</i>	
E19	<i>Fgf10+/-</i>		26F_3(HG+)	Figure S12I, I'	F-actin	
E19	<i>Fgf10+/-</i>		26F_6(HG+)	Figure S11G, H	ISH for <i>Fgf7</i>	
E19	<i>Fgf10+/-</i>		26F_7(no HG)	Figure 4G~L	ISH for <i>Fgf7, Fgf10, Fgfr2b</i>	
E19	<i>Fgf10+/-</i>		26F_7(no HG)	Figure S9	ISH for <i>Fgf10, Fgfr2b</i>	
E19	<i>Fgf10+/-</i>		26F_7(no HG)	Figure S11I, J	ISH for <i>Fgf7</i>	
E19	<i>Fgf10+/-</i>		26F_8(no HG)	Figure S11K, L	ISH for <i>Fgf7</i>	
E19	<i>Fgf10+/-</i>		26F_8(no HG)	Figure S12A~H	ISH for <i>Fgf10, Fgfr2b</i>	
E19	<i>Fgf10+/-</i>		26F_2(no HG)	Figure S12J, J'	F-actin	
E15	WT		36F_1	Figure 2C, C'; Figure S6A, B, A'	HE	
E15	WT		36F_3	Figure S6C, D	HE	
E15	WT		61F_6	Figure S6 E, F, F'	HE	
E15	<i>Fgf10+/-</i>		36F_4	Figure 2D, D'; Figure S6G, H, G'	HE	
E15	<i>Fgf10+/-</i>		36F_6	Figure S6I, J, J'	HE	
E15	<i>Fgf10+/-</i>		61F_3	Figure S6K, L	HE	
E15	<i>Fgf10-/-</i>		61F_5	Figure S6M, N	HE	
E15	<i>Fgf10-/-</i>		61F_7	Figure S6O, P	HE	